

GECO: Generative Image-to-3D within a SECOnd

Chen Wang¹, Jiatao Gu², Xiaoxiao Long³, and Yuan Liu³ and Lingjie Liu¹

¹University of Pennsylvania ²Apple ³The University of Hong Kong

<https://cwchenwang.github.io/geco>

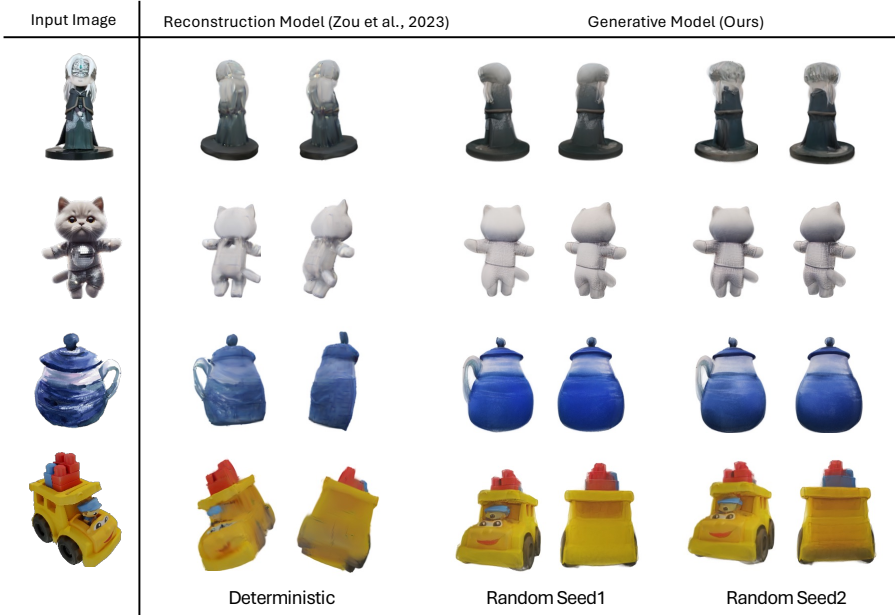


Fig. 1: We propose GECO, a framework for feed-forward 3D generation that can produce 3D Gaussians from random noises in about **0.35 seconds** on a single L40 GPU.

Abstract. 3D generation has seen remarkable progress in recent years. Existing techniques, such as score distillation methods, produce notable results but require extensive per-scene optimization, impacting time efficiency. Alternatively, reconstruction-based approaches prioritize efficiency but compromise quality due to their limited handling of uncertainty. We introduce GECO, a novel method for high-quality 3D generative modeling that operates within a second. Our approach addresses the prevalent issues of uncertainty and inefficiency in current methods through a two-stage approach. In the initial stage, we train a single-step multi-view generative model with score distillation. Then, a second-stage distillation is applied to address the challenge of view inconsistency from the multi-view prediction. This two-stage process ensures a balanced approach to 3D generation, optimizing both quality and efficiency.

Our comprehensive experiments demonstrate that GECO achieves high-quality image-to-3D generation with an unprecedented level of efficiency.

Keywords: Score Distillation · Gaussian Splatting · Image-to-3D

1 Introduction

3D digital assets encapsulate geometry and appearance of objects from the real world. The role of 3D assets is pivotal across a wide range of applications, including movies, digital games, virtual reality, and robotics. Despite their importance, generating 3D assets is often labor-intensive and typically restricted to skilled professionals. Automating the generation of 3D models can significantly simplify the workload and open up the creation process to beginners. In this paper, we study the problem of efficiently producing high-quality 3D assets using a single input image, aiming for fast and faithful reproduction of the original object in the image.

Dreamfusion [46] and the follow-up works [4, 29, 31, 48, 64, 67] propose to distill 3D neural representations [23, 41, 43] from pretrained large-scale 2D diffusion models [49, 50] with score distillation techniques. These methods generate high-quality 3D assets with text or image input, however, facing the major drawback that they require 30 minutes of per-scene optimization for only one object, which raises practical concerns in real-time applications. On the other hand, reconstruction-based models (e.g., PixelNeRF [74], LRM [19], TGS [80]) train a deterministic prediction model for the 3D representation given single image input. By leveraging large-scale 3D datasets, such models exhibit a surprising generalization ability over unseen objects, and only require a single forward to obtain the 3D within a second time-frame. However, even with numerous parameters, the uncertainty issue of a single image to 3D prediction is fundamentally unsolvable for deterministic methods: unseen regions of a 3D object cannot be fully recovered from the single image input, causing blurriness or incorrect geometries (see Fig. 1), especially for unseen regions.

Tackling the uncertainty issues, various methods have been proposed for incorporating generative models such as diffusion models for text-to-3D generation tasks [11, 25, 63]. For instance, LGM [63] employs a multi-view diffusion model [54, 55] to first synthesize multi-view consistent images given the single image, and predict the final 3D representations based on the predicted images. In such case, the uncertainty problem can be alleviated by the first-stage diffusion model, and as a result, the predicted 3D is generally better than pure reconstruction-based models. However, the first stage still takes over 5 seconds due to the iterative sampling nature of diffusion models and thus bottlenecks the applications.

To address these issues, we present GECO, a generative approach that can generate high-fidelity and diverse 3D objects within one second. More specifically, we learn a feed-forward generator similar to reconstruction-based models [19, 80] while taking additional noise as inputs for handling uncertainties. Training such

a model from scratch is a non-trivial task. Instead, we parameterize our model using multi-view images as the intermediate representation, and employ a two-stage distillation approach. For the first stage, we follow variational score distillation (VSD, [67]) and learn a single-step multi-view generator directly from a pre-trained multi-view diffusion model [54]. To obtain the 3D representation from the potentially inconsistent outputs of the first stage, we conduct a second-stage training by jointly finetuning our pretrained single-step multi-view diffusion model from the first stage and a pretrained reconstruction-based method (LGM [63]). We generate pseudo ground truth images using the multi-step diffusion model and the pretrained LGM model for training our second-stage model with reconstruction losses. Notably, this training strategy enables using images from arbitrary viewpoints as supervision for high-quality reconstruction.

We conduct both quantitative and qualitative comparisons on GSO [9] dataset. The results show that our method can well resolve the uncertainty of image-to-3D generation in a highly efficient manner. Compared to previous feed-forward baselines, our method synthesizes high-quality renderings even for the back view of the input object. Experiments for in-the-wild images also demonstrate that GECO produces diverse samples from different noises and achieves better results than other methods.

The contributions of our paper can be summarized as the following:

- We design a feed-forward framework for generative 3D generation that considers the uncertainty and requires no diffusion on 3D representations.
- We propose to use a two-stage distillation method for effectively training the generator from pre-trained diffusion and reconstruction models.
- Extensive experiments demonstrate that our method GECO achieves high-quality 3D generation in less than one second.

2 Preliminaries

2.1 Multi-view Diffusion Models

Diffusion Models [16, 58] learn the data distribution by estimating the noised data distribution (or score) along a Markov Chain. Diffusion models consist of a forward process that gradually removes information from data by adding Gaussian noises and a reverse process that generates data starting from random noise. Given $\mathbf{x}_0 \sim q(\mathbf{x}_0)$, the forward process q is a Markov chain that adds gaussian noise to \mathbf{x}_0 and generates latent $\mathbf{x}_1, \dots, \mathbf{x}_T$ of the same dimension with $q(\mathbf{x}_t|\mathbf{x}) = \mathcal{N}(\alpha_t\mathbf{x}, \sigma_t^2\mathbf{I})$. Ideally, the final latent \mathbf{x}_T will follow a standard Gaussian distribution: $p(\mathbf{x}_T) = \mathcal{N}(\mathbf{x}_T; \mathbf{0}, \mathbf{I})$. The reverse process starts denoising from \mathbf{x}_T by learning the Gaussian transitions from \mathbf{x}_t to \mathbf{x}_{t-1} that is defined as $p_\theta(\mathbf{x}_{0:T}) := p(\mathbf{x}_T) \prod_{t=1}^T p_\theta(\mathbf{x}_{t-1}|\mathbf{x}_t)$. Further, $p_\theta(\mathbf{x}_{t-1}|\mathbf{x}_t) = \mathcal{N}(\mathbf{x}_{t-1}, \mu_\theta(\mathbf{x}_t, t), \sigma_t^2\mathbf{I})$ and μ_θ is the learnable component. The sampling of diffusion models often takes more than 50 steps to obtain high-quality samples.

Multi-view Diffusion Models learn the joint probability distribution of multi-view images [32, 33, 54]. This kind of model treats multi-view renderings of

an object on a fixed set of viewpoints as the data point. The learning process of multi-view diffusion models is similar to standard image diffusion models except that noises are added and denoised simultaneously to those images. They also need special design to maintain the consistency of different viewpoints. However, the problem with these models is that multiple inference steps are required, and the results are not view-consistent enough. Furthermore, post-processing is also needed to reconstruct 3D geometry and appearance from the multi-view image outputs of these models.

2.2 3D Reconstruction Models

Reconstruction models aim to produce 3D representations of an object from a single view or multiple views. PixelNeRF [74] achieves single-view 3D reconstruction by projecting the input image features to 3D and applying volume rendering for learning 3D representations. The recent work, LRM [19], greatly boosts the reconstruction quality of PixelNeRF by leveraging a large transformer model. However, these methods generally synthesize blurry results from unseen viewpoints because they don't model the uncertainty and only use regression loss to train. This issue can be addressed by using multi-view inputs for the reconstruction model. For example, by using multi-view images generated by multi-view diffusion models as the input, the 3D reconstruction model, Instant3D [25] and LGM [63] can reconstruct 3D models from text or image prompts. Specifically, LGM [63] predicts Splatter Image [62] for each input image, which can be directly fused into 3D Gaussians for novel viewpoint rendering.

3 Method

In this section, we introduce GECO – a novel image-to-3D generative model that achieves both efficient sampling and high-quality generation. More precisely, given a single image of an object and a random noise \mathbf{z} , GECO learns a single-step generator to output 3D representations (Splatter Images [62] in our setting) of the object. An illustration of our proposed model is shown in Fig. 2 where multi-view images are used as an intermediate representation similar to [25, 63]. We learn our models efficiently using a two-stage distillation approach given pre-trained multi-view diffusion and reconstruction models, where we first learn an efficient multi-view generator based on variational score distillation (VSD, Sec. 3.1), and then finetune the full model with a 3D consistent distillation algorithm (Sec. 3.2).

3.1 Stage I: Multi-view Score Distillation

Variational Score Distillation (VSD) VSD [67] is an extension of Score Distillation Sampling (SDS), which was first introduced by DreamFusion [46] for distilling pre-trained 2D diffusion knowledge into 3D. The core idea of SDS is to match the score function between the output of a learnable parametric

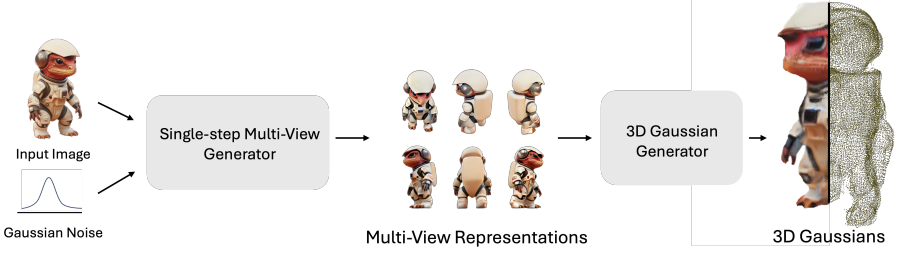


Fig. 2: Overall pipeline of our one-step 3D generator, which achieves image-to-3D Gaussian generation within one second given a conditional image and noise.

image generator and the real data estimated by a pretrained diffusion model. Given a datapoint $\mathbf{x} = g(\theta)$ generated by the differentiable image generator g with parameters θ , SDS adds Gaussian noise of level t and turns it into \mathbf{x}_t . It then uses a pre-trained diffusion model with denoising function $\epsilon_\phi(\mathbf{x}_t; y, t)$ to predict the noise with condition y to optimize θ . ProlificDreamer [67] proposed VSD to further improve SDS by directly optimizing the distribution of θ such that the rendering distribution $q(\mathbf{x}|y)$ with condition y align with the pretrained diffusion model $p(\mathbf{x}|y)$ by minimizing their KL divergence: $D_{\text{KL}}(q(\mathbf{x}|y)||p(\mathbf{x}|y))$. In practice, this is achieved by learning a separate “student model” that estimates the score function of the learned 3D models. The learned score will be used for back-propagation to learn 3D distribution.

Generative Modeling with VSD The original ProlificDreamer parameterized the 3D distribution using a fixed number of particles [67], which, however, does not allow us to draw new samples from the learned distribution. To facilitate learning a 3D generative model that can handle novel scenes, we propose to replace the original parameterization with a learnable generator $\mathcal{G}(\theta)$ that transforms a random Gaussian noise ϵ input to a data sample. The training objective of \mathcal{G} is derived as follows:

$$\nabla_\theta \mathcal{L}_{\text{VSD}} = \mathbb{E}_{t, \epsilon} \left[w(t) (\epsilon_{\text{pre}}(\mathbf{x}_t; y, t) - \epsilon_{\text{stu}}(\mathbf{x}_t; y, t)) \frac{\partial \mathcal{G}(\theta, \mathbf{z})}{\partial \theta} \right] \quad (1)$$

where $\mathbf{x}_0 = \mathcal{G}(\theta, \mathbf{z})$ is the clean sample of the generator output given noise $\mathbf{z} \in \mathcal{N}(0, \mathbf{I})$ and \mathbf{x}_t is the noisy version of \mathbf{x}_0 , t is the diffusion timestep, ϵ_{pre} is the predictions of the pretrained diffusion model. ϵ_{stu} is the predictions of the student model, which is trained online on the output of \mathcal{G} to estimate the score of the generated samples:

$$\mathcal{L}_{\text{stu}} = \mathbb{E}_{t, \epsilon} \|\epsilon_{\text{stu}}(\mathbf{x}_t; y, t) - \epsilon\|_2^2 \quad (2)$$

Multi-view Distillation Ideally, our goal is to learn a 3D generator that maps random noises to 3D representations using VSD, and the 2D renderings of the generator become the input of the 2D diffusion models. Here, we can leverage large-scale pre-trained multi-view diffusion models [33, 54] as our teacher models to improve the learning of 3D inductive bias. A natural design would be

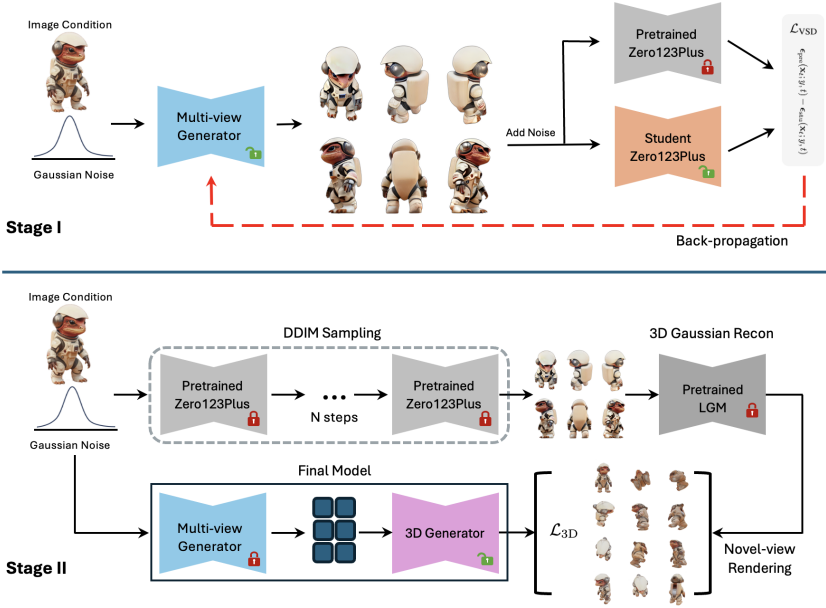


Fig. 3: The two-stage learning pipeline for GECO. Stage I: the multi-view generator is optimized with VSD [67] objective with a pre-trained multi-view diffusion model [54]; Stage II: the full model is optimized by predicting the rendering from the pre-trained reconstruction model [63] under the same image and noise condition.

to parametrize $\mathcal{G}(\theta, \mathbf{z})$ with a 3D generator, such as a triplane generator [3]. However, we found that training a generator from scratch without proper initialization would lead to severe mode collapse, *i.e.* all the samples drawn from the generator will become identical. This observation coincides with the finding in recent work [12, 39, 73] for the distillation of 2D Diffusion models trained on single-view images.

To circumvent this problem, we propose to first learn multi-view images as an intermediate representation using VSD. This allows us to use the same architecture and initial parameters as the pretrained model for our generator \mathcal{G} which is essentially a single-step multi-view generator. In GECO, we employ Zero123Plus [54] as our teacher model because it provides photorealistic and highly consistent 6-view renderings. In contrast to [54] that uses reference attention [75] to concatenate the self-attention matrices of the noised condition image, we directly used the self-attention matrices of the clean condition image to preserve the information. As mentioned earlier, we initialize the generator with Zero123Plus with additional conversion from \mathbf{v} -prediction to \mathbf{x}_0 -prediction.

3.2 Stage II: 3D Consistent Distillation

After the multi-view images of the object are obtained, our next step is to estimate the 3D representation of the object from the multi-view images. One

potential solution is to apply an pretrained 3D reconstruction network \mathcal{R} that takes multi-view images as input and outputs a 3D representation, *i.e.* Splatter Images [62]. However, one major drawback of this approach is that the output of the one-step multi-view generator $\mathcal{G}(\theta)$, which is also the input to the reconstruction network \mathcal{R} , has low multi-view consistency compared to the ground-truth multi-view images, which causes severe training-testing mismatch in the reconstruction model, resulting in blurriness and floating artifacts in the output 3D reconstruction.

As shown in Fig. 3, we propose a second distillation stage to resolve this inconsistency issue, which end-to-end finetunes a reconstruction model as part of the generative model. Considering that the multi-view generation of the teacher diffusion model is much more consistent than the learned single-step generator, we can use the 3D representation reconstructed from these images as pseudo ground truth to further refine our reconstruction model. Namely, given a condition image y and sampled noise \mathbf{z} , we conduct the deterministic DDIM sampling [58] using Zero123Plus [54] to obtain \mathbf{x}_{mv} . 3D Gaussians, represented as Splatter Images, are then reconstructed based on the pretrained 3D reconstructor $\mathcal{R}(\mathbf{x}_{\text{mv}})$. With the reconstructed Gaussians, we render from random viewpoints to create a set of pseudo ground truth images $\{I_i^{\text{syn}}(\mathbf{z}), i = 1, \dots, N\}$. We collect such paired dataset $\mathbf{D} = (\mathbf{z}, \{I_i^{\text{syn}}(\mathbf{z}) | i = 1, \dots, N\})$ for each sampled noise \mathbf{z} , and use them for training the final generator which includes our pretrained single-step multi-view generator (described in Sec. 3.1) and a pretrained 3D reconstructor [63]. Here, $I(\mathbf{z})_i$ represents the i -th view rendered from the generator given \mathbf{z} . In practice, we finetune our final generator by minimizing the difference between the renderings of the generator’s output and the corresponding pseudo ground truth images $\{I_i^{\text{syn}}(\mathbf{z}), i = 1, \dots, N\}$ rendered from the same viewpoint in terms of the RGB loss and LPIPS [76] loss:

$$\mathcal{L}_{3D} = \mathbb{E}_{\mathbf{z}, I^{\text{syn}}(\mathbf{z})} \left[\mathcal{L}_{\text{MSE}}(I_{\text{rgb}}(\mathbf{z}), I_{\text{rgb}}^{\text{syn}}(\mathbf{z})) + \lambda \cdot \mathcal{L}_{\text{LPIPS}}(I_{\text{rgb}}(\mathbf{z}), I_{\text{rgb}}^{\text{syn}}(\mathbf{z})) \right] \quad (3)$$

Note that the 3D reconstructor in the final generator can be regarded as a refinement module that tackles the multi-view inconsistency issue for 3D reconstruction. Furthermore, this training strategy allows us to go beyond the fixed six-view setting specified in Zero123Plus [54] and use the renderings from arbitrary viewpoints for training, which is an important factor for high-quality 3D reconstruction.

4 Experiments

4.1 Implementation Details

Datasets We train our model on the LVIS subset of the Objaverse [7] dataset, which contains approximately 46,000 objects. For each scene, we only need images at one viewpoint to be the condition image of Zero123Plus [54].

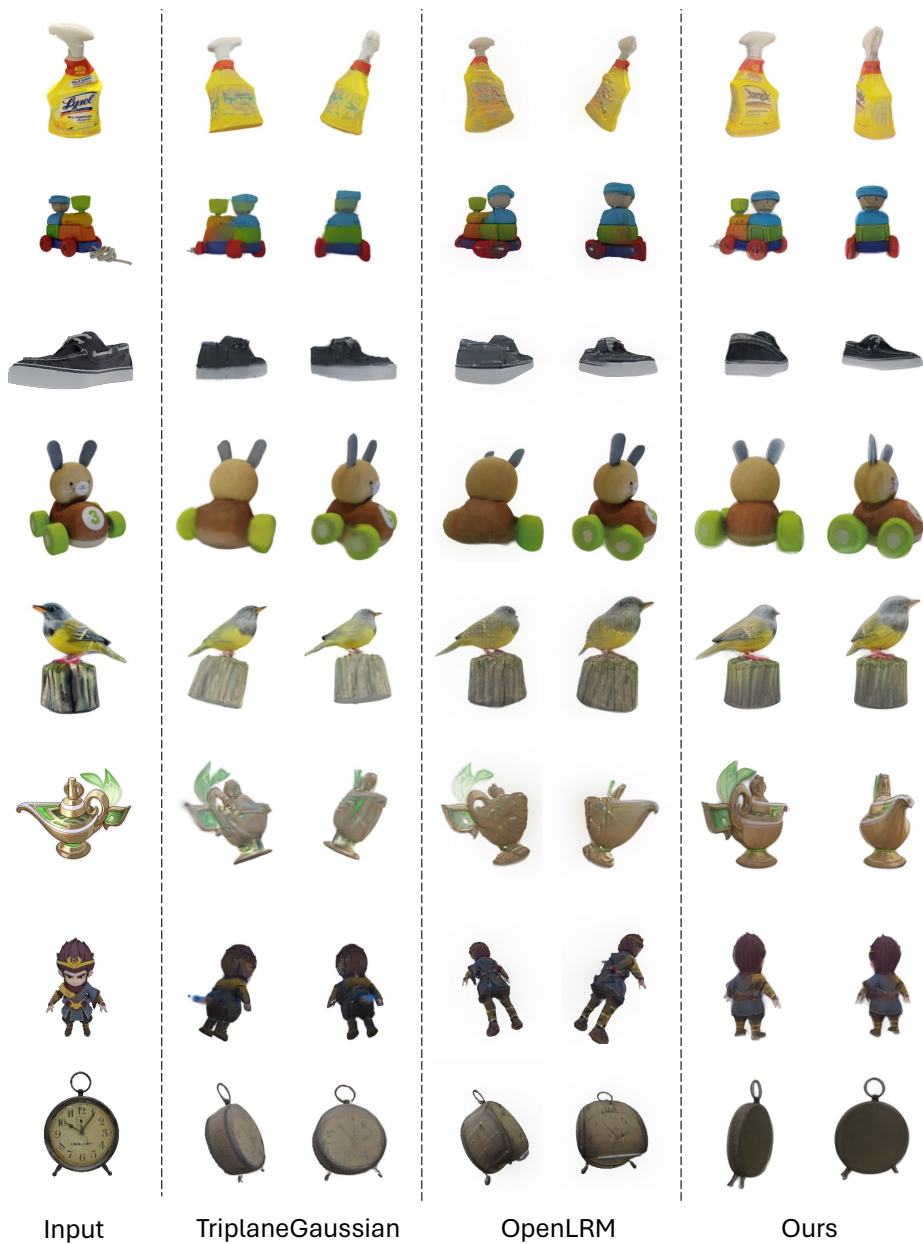


Fig. 4: Qualitative comparison against baseline methods. GECO achieves higher visual quality than the baselines, especially in the unseen view.

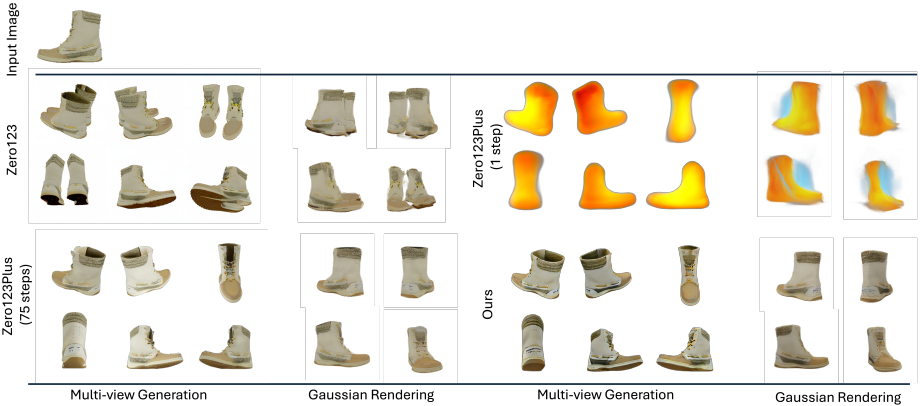


Fig. 5: Comparison of GECO with the baselines that use different multi-view image generation methods and then reconstruct 3D Gaussians. Our one-step multi-view generator produces much better results than Zero123 [31] and is comparable to Zero123Plus [54] 75-step sampling, leading to better 3D Gaussian renderings.

Multi-view Score Distillation For Stage I training, the multi-view generator, pretrained teacher Zero123Plus model, and student Zero123Plus model as shown in Figure 3 are all initialized with Zero123Plus version 1.1 [54]. We train the generator and student model on a single Nvidia L40 GPU for 5,000 steps. For each iteration, the generator and student model are updated alternatively. The t for the student model training is randomly sampled from $[0.02, 0.98]$. We use a fixed guidance scale of 4 for the generator and the pretrained teacher Zero123Plus model, and a guidance scale of 1 for the student model. The generator and the student model are both optimized by the Adam optimizer with learning rate $1e-6$, and betas $(0.9, 0.999)$. We found it is crucial to balance the learning rate of the generator and student model, otherwise, the generator will not converge to reasonable results. The background of input images for Zero123Plus [54] are required to be gray (127 out of 255).

3D Consistent Distillation We adopt LGM [63] as our reconstruction network \mathcal{R} . For each condition image, we ran Zero123Plus with deterministic 75-step DDIM scheduler [58] to obtain the pseudo ground truth six views and use it as input of the LGM [63] model to inference 3D Gaussians. Then we render 50 images at random viewpoints to save them for Stage II training. In Stage II, we use a learning rate of $1e-6$ and a batch size of 8 to train 10 epochs.

Inference The whole pipeline of GECO takes about 0.34s for each scene to generate 3D Gaussians on a single NVIDIA L40 GPU, including 0.28s for multi-view image generation and 0.06s for Gaussian reconstruction. It consumes about 10 GB of GPU memory during inference.

Table 1: Quantitative comparison of novel view synthesis of GECO and the baselines. We report PSNR, SSIM [68], LPIPS [76] on the GSO [9] dataset. The best and second best results are **bolded** and underlined.

Method	PSNR↑	SSIM↑	LPIPS↓	Runtime (s) ↓
Zero123 Sampling [31]	17.28	0.780	0.195	21.0
Zero123 with LGM [31, 63]	17.58	0.777	0.209	21.1
Zero123Plus with LGM [54, 63]	19.03	0.807	<u>0.173</u>	7.12
MVDream with LGM [63]	15.98	0.772	0.222	1.31
TriplaneGaussian [80]	18.52	<u>0.817</u>	0.191	0.13
OpenLRM [13, 19]	18.15	0.810	<u>0.173</u>	3.12
Ours	19.62	0.821	0.159	<u>0.35</u>

4.2 Experiment Protocol

Evaluation Dataset and Metrics Following prior works [30–32], we adopt the Google Scanned Object (GSO) [9] dataset to perform the quantitative comparison of all the methods. We use the same randomly sampled 30 objects ranging from daily objects to animals in SyncDreamer [32]. For each object, we render an image with a size of 256×256 as the input view with zero elevation and render another two sets for evaluation: the first set consists of 6 images from the same viewpoint as in Zero123Plus [54], the second consists of evenly sampled 15 images around the object with zero elevation. We employ commonly used metrics in novel view synthesis for evaluation, including PSNR, SSIM [68] and LPIPS [76].

Baselines We compare with recent methods that focus on feed-forward 3D generation, including LRM [19] and TriplaneGaussian [80]. We use the community version OpenLRM [13] for LRM comparison since the original model is not publicly available. We also include different methods for multi-view image generation, including Zero123 [31], MVDream [55] and Zero123Plus [54]. Then we use LGM [63] to infer 3D Gaussians from the generated multi-view images.

4.3 Results

Qualitative Comparison Figure 4 demonstrates the renderings of GECO and other baselines. We urge readers to view our supplemental video to judge the multi-view consistency of the results. Both our method and TriplaneGaussian achieve highly efficient rendering benefiting from 3D Gaussians, and OpenLRM renders from triplanes, which is much slower. Due to the reconstruction nature, the baseline methods fail to generate reasonable textures at unseen viewpoints, producing flat geometry and blurry renderings. Our method handles the uncertainty through multi-view image generation, so even at the back viewpoints we can synthesize details that are highly consistent with the input image.

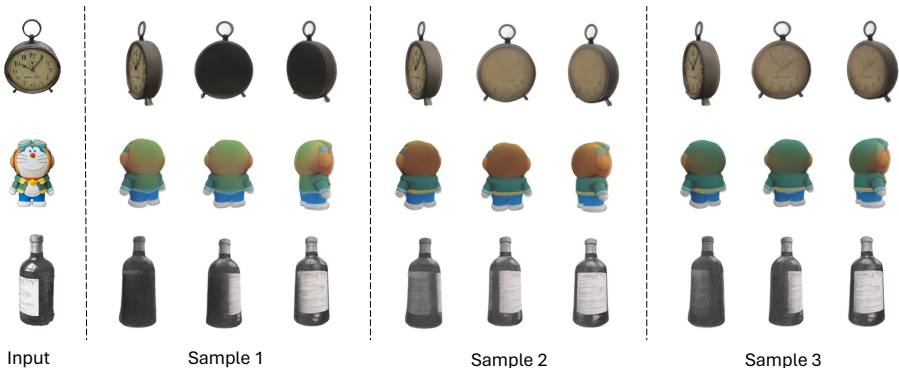


Fig. 6: Given different random seeds, our model produces diverse high-quality 3D Gaussians from the same input image.

Figure 5 further shows comparisons with other methods that also generate multi-view images first and then reconstruct 3D Gaussians. It can be seen from Figure 5 that the output of Zero123 [31] is not consistent across different view-points because each view is generated separately, *e.g.* the shoes are in a pair in one view but not in another. Therefore, the rendered images from 3D Gaussians tend to be blurry. Our method generates multi-view images that are much more consistent and look similar to 75-step sampling of Zero123Plus [54]. The high-quality multi-view generation provides a basis for the 3D generation stage.

Quantitative Comparison The quantitative comparison is shown in Table 1. Our method achieves superior results in major metrics. The improvement results from the uncertainty handling of our approach in the occluded regions. In contrast, TriplaneGaussian [80] and LRM [19] cannot produce sharp predictions for unseen parts, as they are deterministic models. Moreover, we also compare 2D diffusion models for multiview synthesis plus LGM as a 3D reconstructor, we can see our feed-forward model can achieve better or comparable results with those methods that sample multiple steps.

Diversity Thanks to the generative nature of our method, we can produce diverse 3D from different random seeds. As seen from Figure 6, for a single image input, we can generate several reasonable 3D Gaussians in terms of different textures and geometry for the unseen part.

Text-to-image-to-3D Generation Our method can also be combined with text-to-image diffusion models for 3D generation from text prompts. We first use SD-XL [45] to generate images and then run GECO to synthesize 3D. The results are shown in Figure 8.

4.4 Ablation Study

Quality of Multi-View Generator We also evaluated the results of our multi-view image generator on the same GSO [9] dataset we used in Section

Table 2: Quantitatively results on the Gaussian renderings across different settings. We report PSNR, SSIM [68], LPIPS [76] on the GSO [9] dataset.

Method	PSNR \uparrow	SSIM \uparrow	LPIPS \downarrow
1-step Zero123Plus with LGM [54]	12.58	0.665	0.438
Ours w/o Stage II	18.82	0.803	0.174
Ours	19.62	0.821	0.159



Fig. 7: The Stage-II training alleviates the view inconsistency issue in the multi-view diffusion outputs, resulting in higher-quality results with fewer floaters and less over-exposure.

4.2. Results show that our multi-view generator after VSD distillation achieves PSNR/SSIM/LPIPS of 17.73/0.782/0.190, which is very close to the results of 75-step sampling Zero123Plus [54] (17.91/0.789/0.186). From Table 7, we can see that 1-step inference in the original Zero123Plus cannot produce reasonable metrics, while our method is able to generate high-quality 3D Gaussians.

Effectiveness of Stage-II We compare the generation results before and after stage-II training in Figure 7. We can see from the results that after the stage-II training, floating artifacts near the object boundary have gone. This is because the Stage-II training distills a more robust 3D generator that can handle the inconsistency of input images benefiting from the multi-view supervision from the pseudo ground truth images. For Table 2, we can also see that PSNR and SSIM improved after Stage-II and LPIPS nearly remains unchanged.

5 Related Work

Acceleration of Diffusion Models Diffusion Models [8, 16, 58, 60], also known as score-based generative models, achieved tremendous success for various generative tasks, including text [10], image [49, 50], video [15, 17] and 3D [11, 31]. The continuous form of diffusion models are SDEs that transform between data distribution and a prior distribution [60]. The SDEs also have corresponding probability flow ODE with the same marginal distribution [58, 60]. One of the major drawbacks of diffusion models is that they require hundreds of denoising



Fig. 8: Our method also supports 3D generation from text prompts.

steps to generate the final output. Researchers have proposed efficient diffusion samplers [1, 22, 35, 77] to reduce the sampling steps of pretrained diffusion models to less than 50. Another line of works formulates the acceleration problem under the framework of knowledge distillation [14], where a fast student model is distilled from the teacher model. The pioneering work of Salimans and Ho [51] progressively reduces the number of steps for StableDiffusion by training multiple student models. Consistency models [38, 59] and BOOT [12] learn a one-step generator that matches the output of the teacher model along the ODE trajectory at each timestep by bootstrapping in a forward or backward manner respectively. Recently, ADD [53] and DMD [73] introduced score distillation [46, 67] for diffusion distillation.

3D Generation with Diffusion Models Researchers have explored directly training diffusion models on 3D representations, *e.g.* point clouds, triplanes, neural fields [6, 21, 37, 42, 57, 69]. However, they require exhaustive 3D data and computation resources and are also limited to category-level shape generation with simple textures. Other works proposed to learn 3D models from 2D pretrained diffusion models with score distillation [46, 66, 67] by matching the distribution of 3D renderings with that of 2D images. Following up works further improves the quality by using high-resolution guidance [4, 29, 48, 61], disentangling geometry and appearance [4, 48], introducing advanced diffusion guidance [24, 27, 40, 61, 78]. Currently, these methods achieve high-fidelity 3D generation with detailed texture. Besides, the same objective is also widely utilized in scene-level generation [18, 44], 3D editing [26, 79], texturing [40, 72] and articulated object generation [2, 20, 28].

As an intermediate 3D representation, the generation of multi-view images using diffusion models has also been explored. The advantage of multi-view images is that they are batched 2D projects and can be directly processed by existing image diffusion models with minor changes. Existing works [32, 33, 36,

52, 54–56, 65, 70] fine-tuned from pretrained StableDiffusion variants to generate view consistent multi-view images, which is then fused or reconstructed to 3D representations. However, they still require several seconds to perform diffusion sampling and our work addresses this by learning to generate multi-view images in one step.

Efficient 3D Generation Methods based on score distillation often require several minutes of optimization to obtain one 3D model even with efficient 3D representations [5, 64]. Some works [34, 47] use score distillation to train a hypernetwork of neural fields, enabling 3D generation from direct inference but having limited generalization ability. Recently, LRM [19] trains a reconstruction model on large-scale datasets [7] and enables image-to-3D in 5 seconds. Triplane-Gaussian [80] further uses 3D Gaussians to assist the generation of triplanes for LRM. However, the major problem of reconstruction-based methods is that they do not consider the uncertain nature of 3D generation, so the back views of the generated objects are often blurry. Based on LRM, Instant3D [25] first samples multi-view images with 2D diffusion for LRM reconstruction and DMV3D [71] directly trains a 3D diffusion with LRM. Both works improve quality but sacrifice efficiency. Concurrently work LGM [63] designed a 4-view reconstruction model based on Splatter image [62] to achieve ultra-fast multi-view to 3D reconstruction, making the random noise to multi-view image sampling stage become the main bottleneck.

6 Conclusion and Future Work

In this work, we present GECO, a generative framework for 3D content generation. We found that directly learning a 3D generative model that generalizes well involves learning from massive 3D data. Therefore, we use the intermediate representation and employ a multi-view image generation and reconstruction framework. The uncertainty of 3D generation is well addressed in the multi-view image diffusion stage that enjoys the rich prior of pretrained 2D image diffusion models. Then, 3D can be obtained through multi-view reconstruction. We further jointly learn the multi-view image generator and reconstructor to improve the 3D consistency. The whole pipeline is feed-forward and requires less than 0.5 seconds.

Although we have achieved high-quality and efficient 3D generation, our approach still has several limitations. First, our training process involves two stages, including distilling a multi-view image diffusion model and optimizing it with a reconstruction model jointly. Second, the results of our work are bounded by the multi-step sampling results of the multi-view diffusion models, which might still not be as consistent as renderings of 3D representations to produce a clean 3D without floaters. Future work can consider learning a one-step 3D generative model that can produce 3D representations directly, either by training from scratch or distilling a diffusion model.

References

1. Bao, F., Li, C., Zhu, J., Zhang, B.: Analytic-dpm: an analytic estimate of the optimal reverse variance in diffusion probabilistic models. ICLR (2021) **13**
2. Cao, Y., Cao, Y.P., Han, K., Shan, Y., Wong, K.Y.K.: Dreamavatar: Text-and-shape guided 3d human avatar generation via diffusion models. arXiv preprint arXiv:2304.00916 (2023) **13**
3. Chan, E.R., Lin, C.Z., Chan, M.A., Nagano, K., Pan, B., De Mello, S., Gallo, O., Guibas, L.J., Tremblay, J., Khamis, S., et al.: Efficient geometry-aware 3d generative adversarial networks. In: CVPR. pp. 16123–16133 (2022) **6**
4. Chen, R., Chen, Y., Jiao, N., Jia, K.: Fantasia3d: Disentangling geometry and appearance for high-quality text-to-3d content creation. ICCV (2023) **2, 13**
5. Chen, Z., Wang, F., Liu, H.: Text-to-3d using gaussian splatting. arXiv preprint arXiv:2309.16585 (2023) **14**
6. Chou, G., Bahat, Y., Heide, F.: Diffusion-sdf: Conditional generative modeling of signed distance functions. In: CVPR. pp. 2262–2272 (2023) **13**
7. Deitke, M., Liu, R., Wallingford, M., Ngo, H., Michel, O., Kusupati, A., Fan, A., Laforte, C., Voleti, V., Gadre, S.Y., et al.: Objaverse-xl: A universe of 10m+ 3d objects. arXiv preprint arXiv:2307.05663 (2023) **7, 14**
8. Dhariwal, P., Nichol, A.: Diffusion models beat gans on image synthesis. NeurIPS **34**, 8780–8794 (2021) **12**
9. Downs, L., Francis, A., Koenig, N., Kinman, B., Hickman, R., Reymann, K., McHugh, T.B., Vanhoucke, V.: Google scanned objects: A high-quality dataset of 3d scanned household items. In: 2022 International Conference on Robotics and Automation (ICRA). pp. 2553–2560. IEEE (2022) **3, 10, 11, 12**
10. Gong, S., Li, M., Feng, J., Wu, Z., Kong, L.: Diffuseq: Sequence to sequence text generation with diffusion models. ICLR (2023) **12**
11. Gu, J., Trevithick, A., Lin, K.E., Susskind, J.M., Theobalt, C., Liu, L., Ramamoorthi, R.: Nerfdiff: Single-image view synthesis with nerf-guided distillation from 3d-aware diffusion. In: ICML. pp. 11808–11826. PMLR (2023) **2, 12**
12. Gu, J., Zhai, S., Zhang, Y., Liu, L., Susskind, J.M.: Boot: Data-free distillation of denoising diffusion models with bootstrapping. In: ICML 2023 Workshop on Structured Probabilistic Inference & Generative Modeling (2023) **6, 13**
13. He, Z., Wang, T.: Openlrm: Open-source large reconstruction models. <https://github.com/3DTopia/OpenLRM> (2023) **10**
14. Hinton, G., Vinyals, O., Dean, J.: Distilling the knowledge in a neural network. arXiv preprint arXiv:1503.02531 (2015) **13**
15. Ho, J., Chan, W., Saharia, C., Whang, J., Gao, R., Gritsenko, A., Kingma, D.P., Poole, B., Norouzi, M., Fleet, D.J., et al.: Imagen video: High definition video generation with diffusion models. arXiv preprint arXiv:2210.02303 (2022) **12**
16. Ho, J., Jain, A., Abbeel, P.: Denoising diffusion probabilistic models. NeurIPS **33**, 6840–6851 (2020) **3, 12**
17. Ho, J., Salimans, T., Gritsenko, A.A., Chan, W., Norouzi, M., Fleet, D.J.: Video diffusion models. In: ICLR Workshop on Deep Generative Models for Highly Structured Data (2022), <https://openreview.net/forum?id=BBelR2NdDZ5> **12**
18. Höllein, L., Cao, A., Owens, A., Johnson, J., Nießner, M.: Text2room: Extracting textured 3d meshes from 2d text-to-image models. ICCV (2023) **13**
19. Hong, Y., Zhang, K., Gu, J., Bi, S., Zhou, Y., Liu, D., Liu, F., Sunkavalli, K., Bui, T., Tan, H.: Lrm: Large reconstruction model for single image to 3d. ICLR (2024) **2, 4, 10, 11, 14**

20. Jakab, T., Li, R., Wu, S., Rupprecht, C., Vedaldi, A.: Farm3d: Learning articulated 3d animals by distilling 2d diffusion. arXiv preprint arXiv:2304.10535 (2023) **13**
21. Jun, H., Nichol, A.: Shap-e: Generating conditional 3d implicit functions. arXiv preprint arXiv:2305.02463 (2023) **13**
22. Karras, T., Aittala, M., Aila, T., Laine, S.: Elucidating the design space of diffusion-based generative models. *NeurIPS* **35**, 26565–26577 (2022) **13**
23. Kerbl, B., Kopanas, G., Leimkühler, T., Drettakis, G.: 3d gaussian splatting for real-time radiance field rendering. *ACM TOG* **42**(4) (2023) **2**
24. Kwak, J.g., Dong, E., Jin, Y., Ko, H., Mahajan, S., Yi, K.M.: Vivid-1-to-3: Novel view synthesis with video diffusion models. arXiv preprint arXiv:2312.01305 (2023) **13**
25. Li, J., Tan, H., Zhang, K., Xu, Z., Luan, F., Xu, Y., Hong, Y., Sunkavalli, K., Shakhnarovich, G., Bi, S.: Instant3d: Fast text-to-3d with sparse-view generation and large reconstruction model. *ICLR* (2024) **2, 4, 14**
26. Li, Y., Dou, Y., Shi, Y., Lei, Y., Chen, X., Zhang, Y., Zhou, P., Ni, B.: Focaldreamer: Text-driven 3d editing via focal-fusion assembly. arXiv preprint arXiv:2308.10608 (2023) **13**
27. Liang, Y., Yang, X., Lin, J., Li, H., Xu, X., Chen, Y.: Luciddreamer: Towards high-fidelity text-to-3d generation via interval score matching. arXiv preprint arXiv:2311.11284 (2023) **13**
28. Liao, T., Yi, H., Xiu, Y., Tang, J., Huang, Y., Thies, J., Black, M.J.: Tada! text to animatable digital avatars. arXiv preprint arXiv:2308.10899 (2023) **13**
29. Lin, C.H., Gao, J., Tang, L., Takikawa, T., Zeng, X., Huang, X., Kreis, K., Fidler, S., Liu, M.Y., Lin, T.Y.: Magic3d: High-resolution text-to-3d content creation. In: *CVPR*. pp. 300–309 (2023) **2, 13**
30. Liu, M., Xu, C., Jin, H., Chen, L., Varma T, M., Xu, Z., Su, H.: One-2-3-45: Any single image to 3d mesh in 45 seconds without per-shape optimization. *NeurIPS* **36** (2024) **10**
31. Liu, R., Wu, R., Van Hoorick, B., Tokmakov, P., Zakharov, S., Vondrick, C.: Zero-1-to-3: Zero-shot one image to 3d object. In: *ICCV*. pp. 9298–9309 (2023) **2, 9, 10, 11, 12**
32. Liu, Y., Lin, C., Zeng, Z., Long, X., Liu, L., Komura, T., Wang, W.: Syncdreamer: Generating multiview-consistent images from a single-view image. *ICLR* (2024) **3, 10, 13**
33. Long, X., Guo, Y.C., Lin, C., Liu, Y., Dou, Z., Liu, L., Ma, Y., Zhang, S.H., Habermann, M., Theobalt, C., et al.: Wonder3d: Single image to 3d using cross-domain diffusion. arXiv preprint arXiv:2310.15008 (2023) **3, 5, 13**
34. Lorraine, J., Xie, K., Zeng, X., Lin, C.H., Takikawa, T., Sharp, N., Lin, T.Y., Liu, M.Y., Fidler, S., Lucas, J.: Att3d: Amortized text-to-3d object synthesis. arXiv preprint arXiv:2306.07349 (2023) **14**
35. Lu, C., Zhou, Y., Bao, F., Chen, J., Li, C., Zhu, J.: Dpm-solver: A fast ode solver for diffusion probabilistic model sampling in around 10 steps. *NeurIPS* **35**, 5775–5787 (2022) **13**
36. Lu, Y., Zhang, J., Li, S., Fang, T., McKinnon, D., Tsin, Y., Quan, L., Cao, X., Yao, Y.: Direct2. 5: Diverse text-to-3d generation via multi-view 2.5 d diffusion. arXiv preprint arXiv:2311.15980 (2023) **13**
37. Luo, S., Hu, W.: Diffusion probabilistic models for 3d point cloud generation. In: *CVPR*. pp. 2837–2845 (2021) **13**
38. Luo, S., Tan, Y., Huang, L., Li, J., Zhao, H.: Latent consistency models: Synthesizing high-resolution images with few-step inference. arXiv preprint arXiv:2310.04378 (2023) **13**

39. Luo, W., Hu, T., Zhang, S., Sun, J., Li, Z., Zhang, Z.: Diff-instruct: A universal approach for transferring knowledge from pre-trained diffusion models. *NeurIPS* **36** (2024) [6](#)
40. Metzger, G., Richardson, E., Patashnik, O., Giryes, R., Cohen-Or, D.: Latent-nerf for shape-guided generation of 3d shapes and textures. In: *CVPR*. pp. 12663–12673 (2023) [13](#)
41. Mildenhall, B., Srinivasan, P.P., Tancik, M., Barron, J.T., Ramamoorthi, R., Ng, R.: Nerf: Representing scenes as neural radiance fields for view synthesis. *Communications of the ACM* **65**(1), 99–106 (2021) [2](#)
42. Müller, N., Siddiqui, Y., Porzi, L., Bulo, S.R., Kotschieder, P., Nießner, M.: Diffrrf: Rendering-guided 3d radiance field diffusion. In: *CVPR*. pp. 4328–4338 (2023) [13](#)
43. Müller, T., Evans, A., Schied, C., Keller, A.: Instant neural graphics primitives with a multiresolution hash encoding. *ACM TOG* **41**(4), 1–15 (2022) [2](#)
44. Po, R., Wetzstein, G.: Compositional 3d scene generation using locally conditioned diffusion. *arXiv preprint arXiv:2303.12218* (2023) [13](#)
45. Podell, D., English, Z., Lacey, K., Blattmann, A., Dockhorn, T., Müller, J., Penna, J., Rombach, R.: Sdxl: Improving latent diffusion models for high-resolution image synthesis. *arXiv preprint arXiv:2307.01952* (2023) [11](#)
46. Poole, B., Jain, A., Barron, J.T., Mildenhall, B.: Dreamfusion: Text-to-3d using 2d diffusion. *ICLR* (2023) [2](#), [4](#), [13](#)
47. Qian, G., Cao, J., Siarohin, A., Kant, Y., Wang, C., Vasilkovsky, M., Lee, H.Y., Fang, Y., Skorokhodov, I., Zhuang, P., et al.: Atom: Amortized text-to-mesh using 2d diffusion. *arXiv preprint arXiv:2402.00867* (2024) [14](#)
48. Qian, G., Mai, J., Hamdi, A., Ren, J., Siarohin, A., Li, B., Lee, H.Y., Skorokhodov, I., Wonka, P., Tulyakov, S., et al.: Magic123: One image to high-quality 3d object generation using both 2d and 3d diffusion priors. *ICLR* (2024) [2](#), [13](#)
49. Rombach, R., Blattmann, A., Lorenz, D., Esser, P., Ommer, B.: High-resolution image synthesis with latent diffusion models. In: *CVPR*. pp. 10684–10695 (2022) [2](#), [12](#)
50. Saharia, C., Chan, W., Saxena, S., Li, L., Whang, J., Denton, E.L., Ghasemipour, K., Gontijo Lopes, R., Karagol Ayan, B., Salimans, T., et al.: Photorealistic text-to-image diffusion models with deep language understanding. *NeurIPS* **35**, 36479–36494 (2022) [2](#), [12](#)
51. Salimans, T., Ho, J.: Progressive distillation for fast sampling of diffusion models. *ICLR* (2022) [13](#)
52. Sargent, K., Li, Z., Shah, T., Herrmann, C., Yu, H.X., Zhang, Y., Chan, E.R., Lagun, D., Fei-Fei, L., Sun, D., et al.: Zeronvs: Zero-shot 360-degree view synthesis from a single real image. *arXiv preprint arXiv:2310.17994* (2023) [13](#)
53. Sauer, A., Lorenz, D., Blattmann, A., Rombach, R.: Adversarial diffusion distillation. *arXiv preprint arXiv:2311.17042* (2023) [13](#)
54. Shi, R., Chen, H., Zhang, Z., Liu, M., Xu, C., Wei, X., Chen, L., Zeng, C., Su, H.: Zero123++: a single image to consistent multi-view diffusion base model. *arXiv preprint arXiv:2310.15110* (2023) [2](#), [3](#), [5](#), [6](#), [7](#), [9](#), [10](#), [11](#), [12](#), [13](#)
55. Shi, Y., Wang, P., Ye, J., Long, M., Li, K., Yang, X.: Mvdream: Multi-view diffusion for 3d generation. *ICLR* (2024) [2](#), [10](#), [13](#)
56. Shi, Y., Wang, J., Cao, H., Tang, B., Qi, X., Yang, T., Huang, Y., Liu, S., Zhang, L., Shum, H.Y.: Toss: High-quality text-guided novel view synthesis from a single image. *arXiv preprint arXiv:2310.10644* (2023) [13](#)
57. Shue, J.R., Chan, E.R., Po, R., Ankner, Z., Wu, J., Wetzstein, G.: 3d neural field generation using triplane diffusion. In: *CVPR*. pp. 20875–20886 (2023) [13](#)

58. Song, J., Meng, C., Ermon, S.: Denoising diffusion implicit models. ICLR (2021) [3](#), [7](#), [9](#), [12](#)
59. Song, Y., Dhariwal, P., Chen, M., Sutskever, I.: Consistency models. ICML (2023) [13](#)
60. Song, Y., Sohl-Dickstein, J., Kingma, D.P., Kumar, A., Ermon, S., Poole, B.: Score-based generative modeling through stochastic differential equations. ICLR (2021) [12](#)
61. Sun, J., Zhang, B., Shao, R., Wang, L., Liu, W., Xie, Z., Liu, Y.: Dreamcraft3d: Hierarchical 3d generation with bootstrapped diffusion prior. arXiv preprint arXiv:2310.16818 (2023) [13](#)
62. Szymanowicz, S., Rupprecht, C., Vedaldi, A.: Splatter image: Ultra-fast single-view 3d reconstruction. arXiv preprint arXiv:2312.13150 (2023) [4](#), [7](#), [14](#)
63. Tang, J., Chen, Z., Chen, X., Wang, T., Zeng, G., Liu, Z.: Lgm: Large multi-view gaussian model for high-resolution 3d content creation. arXiv preprint arXiv:2402.05054 (2024) [2](#), [3](#), [4](#), [6](#), [7](#), [9](#), [10](#), [14](#)
64. Tang, J., Ren, J., Zhou, H., Liu, Z., Zeng, G.: Dreamgaussian: Generative gaussian splatting for efficient 3d content creation. ICLR (2024) [2](#), [14](#)
65. Tang, S., Chen, J., Wang, D., Tang, C., Zhang, F., Fan, Y., Chandra, V., Furukawa, Y., Ranjan, R.: Mvdifffusion++: A dense high-resolution multi-view diffusion model for single or sparse-view 3d object reconstruction. arXiv preprint arXiv:2402.12712 (2024) [13](#)
66. Wang, H., Du, X., Li, J., Yeh, R.A., Shakhnarovich, G.: Score jacobian chaining: Lifting pretrained 2d diffusion models for 3d generation. In: CVPR. pp. 12619–12629 (2023) [13](#)
67. Wang, Z., Lu, C., Wang, Y., Bao, F., Li, C., Su, H., Zhu, J.: Prolificdreamer: High-fidelity and diverse text-to-3d generation with variational score distillation. NeurIPS **36** (2024) [2](#), [3](#), [4](#), [5](#), [6](#), [13](#)
68. Wang, Z., Bovik, A.C., Sheikh, H.R., Simoncelli, E.P.: Image quality assessment: from error visibility to structural similarity. IEEE TIP **13**(4), 600–612 (2004) [10](#), [12](#)
69. Wu, T., Li, Z., Yang, S., Zhang, P., Pan, X., Wang, J., Lin, D., Liu, Z.: Hyperdreamer: Hyper-realistic 3d content generation and editing from a single image. In: SIGGRAPH Asia 2023 Conference Papers. pp. 1–10 (2023) [13](#)
70. Xie, D., Li, J., Tan, H., Sun, X., Shu, Z., Zhou, Y., Bi, S., Pirk, S., Kaufman, A.E.: Carve3d: Improving multi-view reconstruction consistency for diffusion models with rl finetuning. arXiv preprint arXiv:2312.13980 (2023) [13](#)
71. Xu, Y., Tan, H., Luan, F., Bi, S., Wang, P., Li, J., Shi, Z., Sunkavalli, K., Wetstein, G., Xu, Z., et al.: Dmv3d: Denoising multi-view diffusion using 3d large reconstruction model. ICLR (2024) [14](#)
72. Yeh, Y.Y., Huang, J.B., Kim, C., Xiao, L., Nguyen-Phuoc, T., Khan, N., Zhang, C., Chandraker, M., Marshall, C.S., Dong, Z., et al.: Texturedreamer: Image-guided texture synthesis through geometry-aware diffusion. arXiv preprint arXiv:2401.09416 (2024) [13](#)
73. Yin, T., Gharbi, M., Zhang, R., Shechtman, E., Durand, F., Freeman, W.T., Park, T.: One-step diffusion with distribution matching distillation. arXiv preprint arXiv:2311.18828 (2023) [6](#), [13](#)
74. Yu, A., Ye, V., Tancik, M., Kanazawa, A.: pixelnerf: Neural radiance fields from one or few images. In: CVPR. pp. 4578–4587 (2021) [2](#), [4](#)
75. Zhang, L.: Reference-only control (2022), <https://github.com/Mikubill/sd-webui-controlnet/discussions/1236> [6](#)

76. Zhang, R., Isola, P., Efros, A.A., Shechtman, E., Wang, O.: The unreasonable effectiveness of deep features as a perceptual metric. In: CVPR. pp. 586–595 (2018) [7](#), [10](#), [12](#)
77. Zheng, K., Lu, C., Chen, J., Zhu, J.: Dpm-solver-v3: Improved diffusion ode solver with empirical model statistics. NeurIPS **36** (2024) [13](#)
78. Zhu, J., Zhuang, P., Koyejo, S.: Hifa: High-fidelity text-to-3d generation with advanced diffusion guidance. In: ICLR (2024) [13](#)
79. Zhuang, J., Wang, C., Lin, L., Liu, L., Li, G.: Dreameditor: Text-driven 3d scene editing with neural fields. In: SIGGRAPH Asia 2023 Conference Papers. pp. 1–10 (2023) [13](#)
80. Zou, Z.X., Yu, Z., Guo, Y.C., Li, Y., Liang, D., Cao, Y.P., Zhang, S.H.: Triplane meets gaussian splatting: Fast and generalizable single-view 3d reconstruction with transformers. arXiv preprint arXiv:2312.09147 (2023) [2](#), [10](#), [11](#), [14](#)